Research Article Vol. 60, No. 29 / 10 October 2021 / Applied Optics 9101

applied optics

Spectral reduction model for an echelle spectrometer based on a digital micromirror device and photomultiplier

Yingchao Li,[1] Wenyu Jiang,[1] Chunsheng Li,[1,3] Zhenyu Ma,[2] Yuqing Yang,[1] and Di Tian[1,4]

[1]College of Instrumentation & Electrical Engineering, Jilin University, Changchun, Jilin 130012, China
[2]Grating Technology Laboratory, Changchun Institute of Optics and Fine Mechanics and Physics, Chinese Academy of Sciences, Changchun, Jilin 130033, China
[3]e-mail: lics@jlu.edu.cn
[4]e-mail: tiandi@jlu.edu.cn

Received 30 July 2021; revised 17 September 2021; accepted 17 September 2021; posted 17 September 2021 (Doc. ID 439219); published 6 October 2021

For an echelle spectrometer based on a digital micromirror device and photomultiplier, a lens group is placed in front of the digital micromirror device and used to converge the two-dimensional spectrum and correct aberration. The matching spectral reduction model is deduced by establishing the mathematical models of the imaging mirror and lens group. According to the known wavelength and corresponding coordinates, the refractive index of the prism is fitted, and the spectrum is divided into three parts to calibrate. Experimental results of a mercury lamp show that the maximum deviations of x and y coordinates are 3.4 pixels and 2.3 pixels in the corrected spectral reduction model. The deviations are in the range of the errors permitted, which means the extraction of order and wavelength satisfy the requirement of the spectrometer.

https://doi.org/10.1364/AO.439219

1. INTRODUCTION

An echelle grating is a kind of diffraction grating with low groove densities that is blazed for operation at high orders at high diffraction angles [1]. With the advantages of high resolution, high diffraction efficiency, a broad spectral range and others, the echelle spectrometer has become the key component in spectrometric instruments such as the inductively coupled plasma-atomic emission spectrometer (ICP-AES) [2] and laser-induced breakdown spectrometer (LIBS) [3]. For a conventional echelle spectrometer, echelle grating is employed as the main dispersion element, while a prism or grating is used as a cross-dispersion element. The resulting two-dimensional spectrum is detected by the array detector, such as a charge-coupled device (CCD) array detector [4]. A digital micromirror device (DMD), a kind of micro-optical-electromechanical device, is a two-dimensional array with hundreds of thousands to millions of micromirrors that can be set independently to the "on" or "off" state to switch selected wavelengths towards a single detector [5]. As the DMD has the merits of no external cooling, long lifetime, rapid and individual movement, it has been successfully used as a light modulator in spectroscopy in recent years [6–9]. The echelle spectrometer based on a DMD has the capability of sending random domain of spectrum onto the photomultiplier tube (PMT) and the domain is freely chosen by the user [10]. It means that the spectrometer could provide a flexible alternative under multielement analysis conditions. In Ref. [11], the authors used the multioptimization method to design the optical path of the echelle spectrometer based on DMD, and the result showed that the resolution of the spectrometer reached 0.01 nm. However, the results were based on the simulation by optical software, and the spectral reduction model was not established.

One of the main problems urgently to be solved for the echelle spectrometer based on DMD and PMT is how to reduce the two-dimensional spectrum to one-dimensional spectral information. Thus, a spectral reduction model is needed to establish the relationship between the wavelength and pixel position on the image plane, namely, the micromirror position of the DMD in this paper. Some methods have been proposed to establish this relationship. The ray-tracing method is dependent on the structure of instruments and requires a very large amount of time for computation [12–15]. The mathematical method enhanced the speed of algorithms but failed to achieve the required accuracy [16–19]. In addition, it is difficult to collect all applicable lasers of different wavelengths to conduct the experiment. Then a spectral reduction algorithm based on establishing a simplified optical model was proposed. It is only suitable for the echelle spectrometer with off-axis parabolic mirrors [20–22]. The spectral reduction algorithm for the echelle spectrometer with spherical mirrors as the collimating mirror and focus mirror was established by calculating the offset distance of principal ray on

the image of the CCD. The influence of environmental factors on the optical element was not considered [23].

In this paper, the echelle spectrometer based on DMD and PMT is first constructed. The matching spectral reduction model is established and corrected. Considering the requirement of a wide wavelength range, we choose the DMD with the existing maximum size for the spectrometer. A lens group placed in front of the DMD is employed to correct aberration, and, more importantly, to converge the two-dimensional spectrum to make sure that it is focused on the area of the DMD. The added lens group increases the complexity of the spectral reduction model. The design parameters of the optical system are the input parameters and the correspondence between the wavelength and spot position on each surface of the optical element are the output parameters in the model. The coordinates of wavelengths for five element lamps (As, Bi, Cd, Pb, Sn) are extracted according to the centroid method by setting the DMD in block scanning mode. Based on these coordinates, the initial spectral reduction model is corrected by fitting the expression of the refractive index and calibrating the free spectrum region divided into three parts. The theoretical and experimental results verify that the pixel deviation of the echelle and prism direction is in the range of the errors permitted.

2. PRINCIPLE OF THE ECHELLE SPECTROMETER BASED ON DMD AND PMT

The optical layout of an echelle spectrometer based on DMD and PMT is shown in Fig. 1. First, an incident light beam passes through the entrance slit; then it is collimated by a spherical mirror. A group of optical lenses, including a cylindrical lens and a spherical mirror, are placed between the entrance slit and collimating mirror, which are used to compensate for astigmatism and spherical aberration. Next, the parallel light beam is dispersed in the longitudinal and transverse direction by an echelle grating and reflective prism, respectively. Then, it is reflected by an imaging mirror and focused on the DMD in the meridian direction through the backend optical lenses. This lens group corrects aberration and converges the two-dimensional spectrum and make sure that the two-dimensional spectrogram is not imaged out of the range of the DMD. Finally, the corresponding wavelength domain is sent to the detector passing through the focusing mirror and focusing lens when the mirrors of DMD are in the ON state.

The DMD used in this work is 0.95 1080p DMD (Texas Instruments, USA; the cover window is replaced by Corning 7980 standard-grade fused silica; the transmittance is beyond 90% in the range of 180–800 nm) with 1920 × 1080 micromirrors, in which each micromirror can rotate +12°(ON state) or −12°(OFF state) from the neutral position and is controlled by a development kit (developed by our research group). Each rectangular block of micromirrors of partial regional DMD corresponds to a small wavelength range, which makes the DMD like an exit slit of adjustable size. The Hamamatsu R955 PMT with a spectral response of 160–900 nm is used for detection.

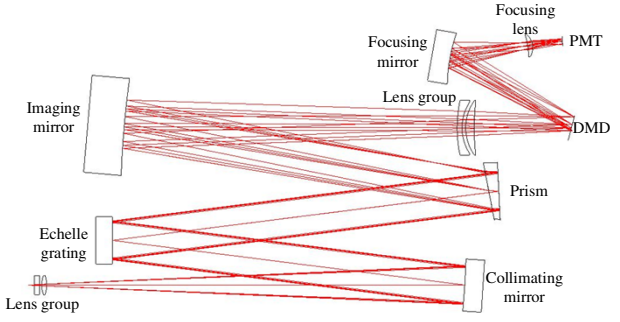

Fig. 1. Optical layout of echelle spectrometer based on DMD and PMT.

3. ESTABLISHMENT OF THE SPECTRAL REDUCTION MODEL

The two-dimensional spectrogram of the free spectrum region is focused and imaged on the DMD after the cross-dispersion. The echelle dispersion is in the vertical (Y) direction, while the prism dispersion is in the horizontal (X) direction. The purpose of establishment of the spectral reduction model is to obtain the relationship between wavelength and the micromirror coordinate. Finally, a one-dimensional spectrogram between wavelength and spectral intensity can be obtained after the detection by the PMT. The offset distance of random wavelength λ from the location of center wavelength in the image plane is calculated as follows.

A. Basic Equations of Two Dispersion Dimensions

The prism used in our design is a reflecting prism; hence, the outgoing angle of the prism i' can be expressed as

$$i' = \arcsin\left[n_1 \cdot \sin\left(2t - \arcsin\frac{\sin k}{n_1}\right)\right], \tag{1}$$

where t is the apex angle of prism, and k is the incident angle of the prism. As the refractive index of prism n_1 is the function of wavelength λ, the one-to-one corresponding relationship can be obtained between wavelength and the x coordinate.

The echelle grating is under the condition of a quasi-Littrow configuration; therefore, the grating equation can be expressed as follows:

$$m\lambda = d\,(\sin i + \sin\theta_\lambda)\cos\omega, \tag{2}$$

where m is the order number, λ is the wavelength, d is the groove spacing, i is the angle of incidence, θ_λ is the angle of diffraction, and ω is the off-axis angle of grating. The diffraction angle of each center wavelength is equal to the incident angle of grating, while that of the other wavelengths are not. θ_λ is the function of wavelength λ, and the height of the light spot on the image plane is the function of θ_λ. Therefore, the one-to-one correspondence between wavelength and y coordinate can be deduced.

The geometric model between imaging mirror and DMD is established as in Fig. 2. O is the spherical center of the imaging

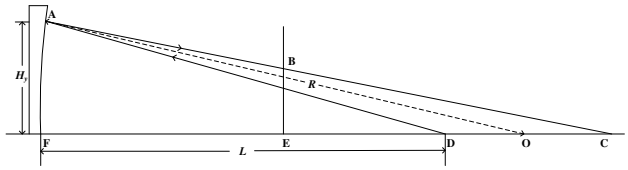

Fig. 2. Geometric model between imaging mirror and DMD.

mirror. OA is the curvature radius of the imaging mirror and equal to the R. DA is the incident light from the front surface of the echelle grating. BE represents the DMD. B is the intersection point of the reflected light and the DMD. Although the light of different wavelengths is diffracted on different positions of the grating, DF is approximately set as the light path from the center of the grating to the center of the imaging mirror, namely L. AF is approximately perpendicular to OF because of the much larger curvature radius of the imaging mirror than its diameter. Hence, $\angle ADF$ and H_y can be written as Eqs. (3) and (4). $\angle ADF$ is also represented by $\Delta\theta_\lambda$,

$$\angle ADF = \theta_\lambda - i = \Delta\theta_\lambda \tag{3}$$

$$H_y = L \cdot \tan \Delta\theta_\lambda. \tag{4}$$

From the exterior angle formula and reflection law, we obtain the following identities:

$$\angle ADF = \angle DAO + \angle AOD, \tag{5}$$

$$\angle AOF = \angle OAC + \angle ACF, \tag{6}$$

$$\angle DAO = \angle OAC. \tag{7}$$

From the above identities, $\angle ACF$ is expressed as follows and is also represented by the symbol σ:

$$\angle ACF = 2\angle AOF - \angle ADF$$

$$= 2 \arcsin \frac{H_y}{R} - \Delta\theta_\lambda. \tag{8}$$

In order to lessen the size of the two-dimensional spectrogram, a group of two spherical mirrors are placed between the imaging mirror and the DMD. The geometric models between the imaging mirror, the group of optical lenses, and the DMD are described in the following section.

B. From Imaging Mirror to the First Spherical Mirror

The geometric model between the imaging mirror and the first spherical mirror in the dispersing direction of the echelle grating is shown in Fig. 3. To simplify the process of calculation, the moving horizontal distance of different wavelengths is approximately the same value, d_1 to d_5. d_1 is the distance between the imaging mirror and the first spherical mirror. d_2 and d_4 are the thickness of the first and second spherical mirrors. The distance between the two spherical mirrors is d_3. d_5 is the distance from the second spherical mirror to the DMD. The offset distance from the location of the center wavelength on the front surface of the first spherical mirror in the vertical direction, y_1, can be expressed by

$$y_1 = H_y - d_1 \cdot \tan\sigma. \tag{9}$$

The curvature radius of the front and back surface of the first spherical mirror are R_1 and R_2, respectively. O_1 and O_2 are spherical centers. The incident angles of the front and back surfaces are φ_1 and φ_3, while the corresponding refracted angles are φ_2 and φ_4. As the first spherical mirror is made of the same material as the prism, its refractive index is shown as n_1. From geometrical considerations, we can get the following equations:

$$\varphi_1 = \arcsin\tfrac{y_1}{R_1} - \sigma, \tag{10}$$

$$\varphi_2 = \arcsin\frac{\sin\varphi_1}{n_1}, \tag{11}$$

$$\xi = \arcsin\frac{y_1}{R_1} - \varphi_2. \tag{12}$$

Based on the sine rule for the corresponding triangle and geometric relationship, the refracted angle φ_3 can be calculated by the following identities:

$$O_1O_2 = R_1 - R_2 - d_2, \tag{13}$$

$$O_1G = \frac{y_1}{\tan\xi} - \sqrt{{R_1}^2 - {y_1}^2}, \tag{14}$$

$$R_2 \cdot \sin\varphi_3 = (O_1O_2 + O_1G) \cdot \sin\xi. \tag{15}$$

The offset distance from the location of center wavelength on the back surface, y_2, can be written as

$$y_2 = R_2 \cdot \sin(\xi + \varphi_3). \tag{16}$$

The geometric model between the imaging mirror and the first spherical mirror in the dispersing direction of the prism

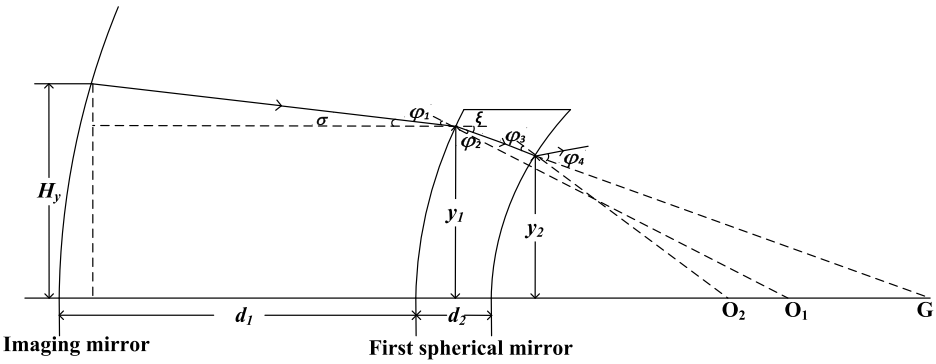

Fig. 3. Geometric model between imaging mirror and the first spherical mirror in the dispersing direction of the echelle grating.

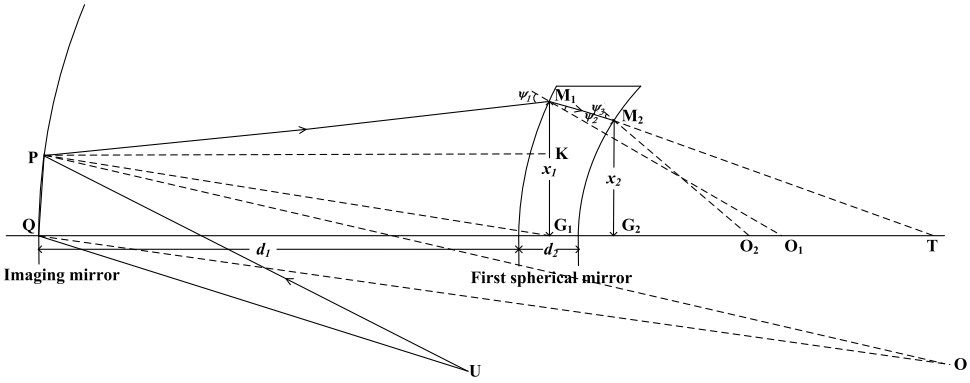

Fig. 4. Geometric model between imaging mirror and the first spherical mirror in the dispersing direction of the prism.

is shown in Fig. 4. U is the origin point of the prism, and i_0 is the angle of the outgoing light of the prism at the center of wavelength. The angle between the random outgoing light of prism and the outgoing light at the center of prism is $\angle QUP$, which can be expressed as

$$\angle QUP = i' - i_0. \tag{17}$$

There are three approximations introduced in order to simplify the process of calculation. First, the light path UQ is approximately equal to the distance L' from the center of prism to the center of the imaging mirror. Second, PQ is approximately perpendicular to QT, as the curvature radius of the imaging mirror is much larger than its diameter. As $\angle UQT$ is very small, PQ is also perpendicular to OQ and UQ. Third, PK, QG_1 is approximately equal to d_1. Based on the above, we can derive

$$\angle QOP = \arctan\frac{L' \cdot \tan\angle QUP}{R}. \tag{18}$$

From the reflection law and the internal angle relations of the triangle, the identities can be deduced as follows:

$$\angle UPO = \angle M_1PO, \tag{19}$$

$$\angle UPO + \angle QOP = \angle UQO + \angle QUP, \tag{20}$$

$$\angle UPO + G_1PO + \angle PG_1Q = 2\angle UQO + \angle QUP. \tag{21}$$

Based on the above identities, $\angle M_1PK$ can be described as

$$\begin{aligned}\angle M_1PK &= \angle UPO - \angle G_1PO - \angle PG_1Q \\ &= \angle QUP - 2\angle QOP.\end{aligned} \tag{22}$$

The offset distance from the location of center wavelength on the front surface of the first spherical mirror in the horizontal direction is expressed by

$$x_1 = d_1 \cdot \tan\angle M_1PK + L' \cdot \tan\angle QUP. \tag{23}$$

The incident angles of the front and back surface are ψ_1 and ψ_3, while the corresponding refracted angles are ψ_2 and ψ_4. The angles can be written as follows:

$$\psi_1 = \arcsin\tfrac{x_1}{R_1} + \angle M_1PK, \tag{24}$$

$$\psi_2 = \arcsin\frac{\sin\psi_1}{n_1}. \tag{25}$$

From the exterior angle formula and law of sines, we can derive the following equations:

$$\angle M_1TG = \arcsin\frac{x_1}{R_1} - \psi_2, \tag{26}$$

$$x_1 = TG_1 \cdot \tan\angle M_1TG_1, \tag{27}$$

$$(TG_1 - O_1G_1 + O_1O_2) \cdot \sin\angle M_1TG_1 = R_2 \cdot \sin\psi_3. \tag{28}$$

Then the incident angle ψ_3 can be calculated. In the horizontal direction, the offset distance from the location of center wavelength on the back surface can be expressed as

$$x_2 = R_2 \cdot \sin(\psi_3 + \angle M_1TG_1). \tag{29}$$

C. From the Second Spherical Mirror to the DMD

The geometric model between the second spherical mirror and the DMD in the dispersing direction of the echelle grating is shown in Fig. 5. O_3 and O_4 are spherical centers. R_3 and R_4 are the curvature radius of the front and back surfaces of the second spherical mirror. The refracted angle φ_4 and angle ε can be expressed as

$$\varphi_4 = \arcsin(n_1 \cdot \sin\varphi_3), \tag{30}$$

$$\varepsilon = \varphi_4 - \arcsin\tfrac{y_2}{R_2}. \tag{31}$$

Based on the sine rule for the corresponding triangles and geometric relationship, the following identities can be obtained and angle γ can be derived:

$$O_2O_3 = R_3 - R_2 + d_2, \tag{32}$$

$$R_2 \cdot \sin\varphi_4 = S_1O_2 \cdot \sin\varepsilon, \tag{33}$$

$$R_3 \cdot \sin(\varepsilon + \gamma) = (S_1O_2 + O_2O_3) \cdot \sin\varepsilon. \tag{34}$$

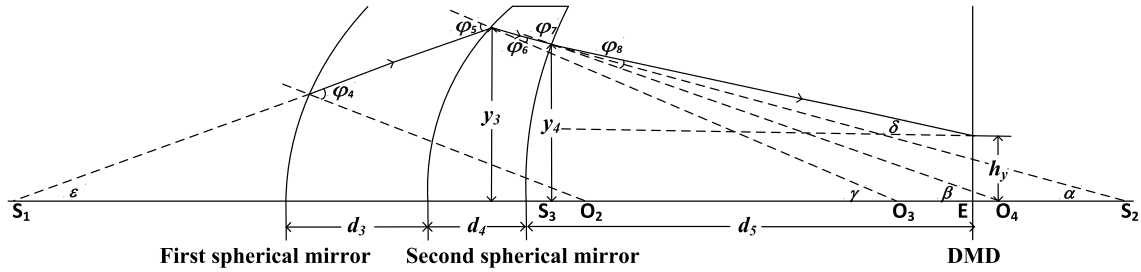

Fig. 5. Geometric model between the second spherical mirror and DMD in the dispersing direction of the echelle grating.

The offset distance from the location of the center wavelength on the front surface of the second spherical mirror can be represented as

$$y_3 = R_3 \cdot \sin\gamma. \tag{35}$$

The incident angles of the front and back surfaces are φ_5 and φ_7, while the corresponding refracted angles are φ_6 and φ_8. n_2 is the refractive index of the second spherical mirror, which is calculated by polynomial fitting. The steps are similar as above. The incident angle φ_5, refracted angle φ_6, and angle α can be expressed as

$$\varphi_5 = \gamma + \varepsilon, \tag{36}$$

$$\varphi_6 = \arcsin\frac{\sin\varphi_5}{n_2}, \tag{37}$$

$$\alpha = \varphi_5 - \varphi_6 - \varepsilon. \tag{38}$$

Then the following identities are acquired and the angle β is calculated:

$$O_3O_4 = R_4 - R_3 + d_3, \tag{39}$$

$$R_3 \cdot \sin\varphi_6 = S_2O_3 \cdot \sin\alpha, \tag{40}$$

$$R_4 \cdot \sin(\beta - \alpha) = (S_2O_3 - O_3O_4) \cdot \sin\alpha. \tag{41}$$

Therefore, the offset distance from the location of the center wavelength on the back surface of the second spherical mirror is written as

$$y_4 = R_4 \cdot \sin\beta. \tag{42}$$

From the exterior angle formula for the corresponding triangles and refraction law, the incident angle φ_7, refracted angle φ_8, and angle δ can be expressed as

$$\varphi_7 = \beta - \alpha, \tag{43}$$

$$\varphi_8 = \arcsin(n_2 \cdot \sin\varphi_7), \tag{44}$$

$$\delta = \beta - \varphi_8. \tag{45}$$

Finally, the height of the light spot on the DMD can be obtained based on above known equations. The relationship between wavelength λ and the y coordinate is given by Eq. (46),

$$\begin{aligned} h_y &= y_4 - S_3E \cdot \tan\delta \\ &= y_4 - [d_5 - (R_4 - R_4 \cdot \cos\beta)] \cdot \tan\delta. \end{aligned} \tag{46}$$

The geometric model between the second spherical mirror and the DMD in the dispersing direction of the prism is shown in Fig. 6. The refracted angle ψ_4 and $\angle M_2VG_2$ are written as

$$\psi_4 = \arcsin(n_1 \cdot \sin\psi_3), \tag{47}$$

$$\angle M_2VG_2 = \psi_4 - \arcsin\frac{x_2}{R_2}. \tag{48}$$

From the law of sines, we can derive the following equations:

$$R_2 \cdot \sin\psi_4 = VO_2 \cdot \sin\angle M_2VG_2, \tag{49}$$

$$R_3 \cdot \sin\angle VM_3O_3 = (VO_2 + O_2O_3) \cdot \sin\angle M_2VG_2. \tag{50}$$

The angle $\angle VM_3O_3$ is calculated, and thus we get the offset distance from the location of the center wavelength on the front surface,

$$x_3 = R_3 \cdot \sin(\angle VM_3O_3 + \angle M_2VG_2). \tag{51}$$

The incident angle ψ_5, refracted angle ψ_6, and the angle $\angle M_4WG_4$ can be expressed as

$$\psi_5 = \pi - \angle VM_3O_3, \tag{52}$$

$$\psi_6 = \arcsin\frac{\sin\psi_5}{n_2}, \tag{53}$$

$$\angle M_4WG_4 = \psi_5 - \psi_6 - \angle M_2VG_2. \tag{54}$$

Next, the steps are similar as above. From the law of sines, we obtain

$$R_3 \cdot \sin\psi_6 = WO_3 \cdot \sin\angle M_4WG_4, \tag{55}$$

$$R_4 \cdot \sin\psi_7 = (WO_3 - O_3O_4) \cdot \sin\angle M_4WG_4. \tag{56}$$

Combined with the above equations, the incident angle ψ_7 is derived, and ψ_8 is described as Eq. (57). The offset distance from the location of the center wavelength on the back surface of the second spherical mirror can be obtained,

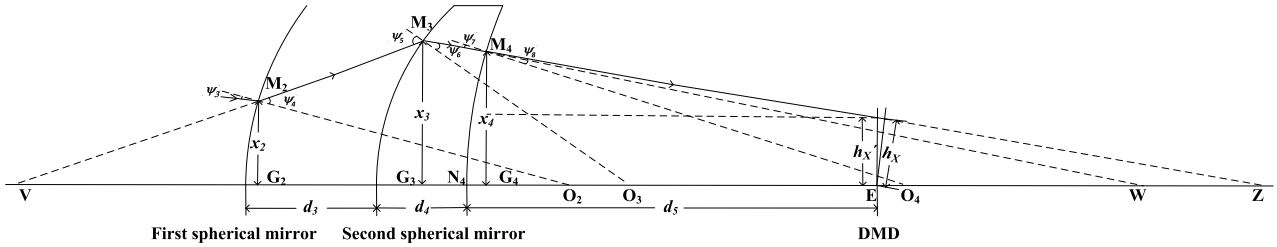

Fig. 6. Geometric model between the second spherical mirror and DMD in the dispersing direction of the prism.

$$\psi_8 = \arcsin(n_2 \cdot \sin\psi_7), \tag{57}$$

$$\begin{aligned} x_4 &= R_4 \cdot \sin\angle M_4 O_4 G_4 \\ &= R_4 \cdot \sin(\psi_7 + \angle M_4 W G_4). \end{aligned} \tag{58}$$

If the DMD is parallel to M_4G_4, the horizontal distance of the light spot on the DMD h'_x can be deduced based on above known equations,

$$\begin{aligned} h'_x &= x_4 - G_4 E \cdot \tan\angle M_4 Z G_4 \\ &= x_4 - (d_5 - G_4 N_4)\tan\angle M_4 Z G_4 \\ &= x_4 - (d_5 - R_4 + R_4 \cdot \cos\angle M_4 O_4 G_4) \\ &\quad \times \tan(\angle M_4 O_4 G_4 - \psi_8). \end{aligned} \tag{59}$$

In the process of detection, each micromirror rotates $+12°$ or $-12°$ from the neutral position. In order to guarantee all spectral information is reflected to the focusing mirror, the DMD is placed at an angle of angle η in the horizontal direction. Therefore, the relationship between wavelength λ and x coordinate is given by Eq. (60),

$$h_x = \frac{h'_x \cdot \cos\angle M_4 Z G_4}{\cos(\eta - \angle M_4 Z G_4)}. \tag{60}$$

A combination of Eqs. (46) and (60) gives the corresponding coordinates on DMD of different wavelengths. The initial theoretical spectral reduction model is established based on the geometric models. For different designs of a reflective-prism echelle spectrometer, the corresponding spectral reduction model can be obtained by substituting the design parameters of the optical elements. As each micromirror acts as a spatial optical switch, S_{xy} is the state of each micromirror, which equals to 1 at the ON state and 0 at the OFF state. I_{xy} is the spectral intensity of each micromirror. The intensity obtained after the detection by PMT is I, shown as Eq. (61), where p and q are the row and column number of the DMD,

$$I = \begin{bmatrix} S_{x_1y_1} \\ S_{x_1y_2} \\ \vdots \\ S_{x_py_q} \end{bmatrix}^T \cdot \begin{bmatrix} I_{x_1y_1} \\ I_{x_1y_2} \\ \vdots \\ I_{x_py_q} \end{bmatrix}. \tag{61}$$

4. CORRECTION OF THE SPECTRAL REDUCTION MODEL

There is a deviation between the actual parameters and the design parameters of the optical system due to the change of ambient temperature and humidity and errors of installation and machining. After the precise adjustment of the spectrometer, the actual coordinate of the wavelength is still not consistent with its theoretical coordinate. It is necessary to correct the initial spectral reduction model and make it match the actual condition of the spectrometer. The steps of the correction of the spectral reduction model are as follows.

A. Fitting the Expression of Refractive Index

The accuracy of the refractive index of the prism has a great influence on the calculation of horizontal coordinates. With the change of the external environment, the refractive index changes. According to the coordinates of known wavelengths in the prism direction, the actual fitting expression for the relationship between the refractive index and the wavelength is obtained. The theoretical expression of the prism in the initial reduction model is substituted by the fitting expression. The Sellmeier method for the relationship between refractive index and wavelength is used and shown in Eq. (62),

$$n(\lambda)^2 - 1 = \frac{{B_1}^2}{\lambda^2 - C_1} + \frac{{B_2}^2}{\lambda^2 - C_2} + \frac{{B_3}^2}{\lambda^2 - C_3}, \tag{62}$$

where $n(\lambda)$ is the refractive index of different wavelengths, and B_1, B_2, B_3 and C_1, C_2, C_3 are coefficients.

In order to fit the actual expression of the refractive index, As, Bi, Cd, Pb, and Sn lamps are used as the light source. First, the two-dimensional spectrograms of element lamps are acquired by setting the DMD in global scanning mode. Then, according to the position of light spots in two-dimensional spectrograms, the corresponding micromirror is set in block scanning mode. In order to obtain a relatively higher signal intensity, the number of simultaneous rotating rows and columns is four micromirrors. For the accuracy of extraction of the coordinate, the number of interval rotating rows and columns is one micromirror. Finally, actual 22 x and y coordinates of corresponding wavelengths for five element lamps are extracted according to the centroid method. The x coordinates are used to deduce the actual refractive index of the position. The fitted coefficients are shown in Table 1.

Table 1. Coefficients for the Expression of Refractive Index

B_1	B_2	B_3	C_1	C_2	C_3
0.6699	0.4332	0.4399	0.0057	0.0120	64.4945

B. Calibration of the Coordinates Expression

The deviation in the direction of the prism increases from the center to the sides of the edge of the DMD because of the spectral line bending resulting from the reflecting prism. As there is no deviation caused by spectral line bending on the center wavelength of each order, the free spectrum region is divided into three parts to calibrate so that the established model is much closer to the actual condition. The bending spectral lines of each order are symmetric about the center and the y theoretical coordinate of center wavelength is 1005, so the adjacent 130 pixels above and below are selected as the part without calibration. Figure 7 is the simulation result of the spectral reduction model imaged on the DMD. The dispersion direction of the prism (x axis) is perpendicular to the dispersion direction of the echelle grating (y axis). The wavelength range is from 190 to 794 nm, and each point corresponds to a small wavelength band. The y coordinate ranges from 1 to 1920, and the x coordinate ranges from 1 to 1080. The sampling interval is set to half of the minimum value for the designed spectral resolution, namely, 0.00185 nm. Based on the known wavelengths of element lamps mentioned above and the corresponding actual coordinates, the expression can be deduced as

$$X = a_i x + b_i, \tag{63}$$

$$Y = c_i y + d_i, \tag{64}$$

where a_i and c_i are the scale coefficients and b_i and d_i are the translation coefficients. (X, Y) is the actual coordinate of the corresponding wavelength while (x, y) is the theoretical coordinate in the spectral reduction model. The value of the element 'i' is I, II, and III, which represents the three parts of the free spectrum region. The scale coefficients and translation coefficients are shown in Table 2.

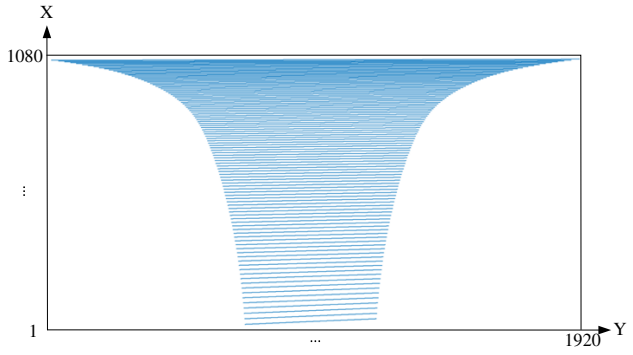

Fig. 7. Simulation result of the spectral reduction model on the DMD.

Table 2. Scale Coefficients and Translation Coefficients of Three Parts

Part	a	b	c	d
I	0.9957	−0.2524	0.9999	−0.0649
II	1	0	1	0
III	0.9963	−0.0396	1.0001	−0.0236

5. RESULTS AND DISCUSSION

The echelle spectrometer developed by our research group is used for the following experiments. The relative design parameters of the echelle spectrometer are shown in Table 3. A mercury lamp is chosen as the light source to verify the accuracy of the spectral reduction model and the precision of the adjustment of instrument. The two-dimensional spectrogram of the mercury lamp is obtained by setting the DMD in global scanning mode, as shown in Fig. 8. In order to quickly obtain a clear image of light spots, the number of simultaneous rotating rows and columns is set to eight micromirrors, and the number of interval rotating rows and columns is set to four micromirrors. Several light spots are marked with their wavelength and labeled by colored boxes. The brightness value of the light spot is the light intensity value of the corresponding characteristic wavelength while the position can be expressed by x and y coordinates.

Based on the coordinates of corresponding wavelengths in the corrected spectral reduction model, the two-dimensional spectrogram of eight wavelengths of mercury lamp are acquired by setting the DMD in block scanning mode. Then the actual coordinates can be obtained by the centroid extraction algorithm. The theoretical coordinates and corrected coordinates can be calculated according to the initial and corrected spectral reduction model, respectively. The contrast results are shown in Table 4. The comparison between the deviation of the corrected spectral reduction model and maximum deviation is shown in Fig. 9. From the results we can summarize that (1) by comparing

Table 3. Parameters of the Echelle Spectrometer

Parameters	Value
Focus length	385 mm
Groove density of echelle	54.5 gr/mm
Incident angle of echelle	46.6°
Offset angle of echelle	7.2°
Apex angle of prism	8.3°
Micromirror size	10.8 μm
Entrance slit	10 × 40 μm

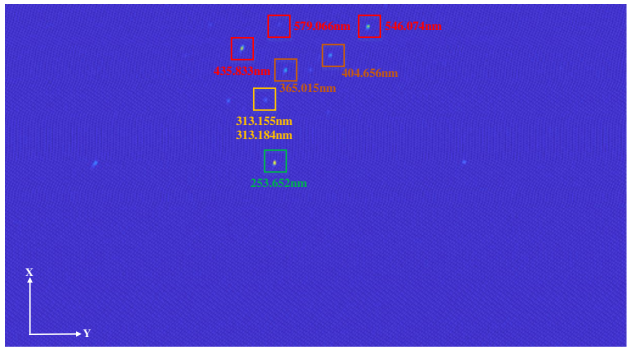

Fig. 8. Two-dimensional spectrogram imaged on DMD.

Table 4. Contrast Results between Actual and Theoretical Coordinate of a Mercury Lamp

Wavelength (nm)	Order	Actual Coordinate	Theoretical Coordinate	Corrected Coordinate	Resolution (nm/pixel)	Interval Pixels between Adjacent Orders
253.652	105	(581.9, 1115.0)	(578.5, 1117.4)	(578.5, 1115.9)	0.0038	11.80
313.155	85	(778.3, 1149.3)	(781.2, 1153.5)	(779.5, 1149.9)	0.0048	8.46
313.184	85	(779.1, 1144.0)	(781.3, 1147.5)	(779.5, 1143.8)	0.0048	8.46
365.015	73	(872.3, 1080.6)	(872.6, 1084.0)	(872.6, 1079.8)	0.0056	6.72
404.656	66	(919.8, 931.7)	(918.1, 934.5)	(919.7, 934.0)	0.0062	6.01
435.833	61	(942.0, 1223.0)	(945.4, 1231.2)	(943.1, 1224.3)	0.0067	5.56
546.074	49	(1009.8, 807.8)	(1006.0, 811.2)	(1008.0, 807.9)	0.0084	4.30
579.066	46	(1017.8, 1098.7)	(1017.7, 1105.8)	(1017.7, 1096.8)	0.0089	4.20

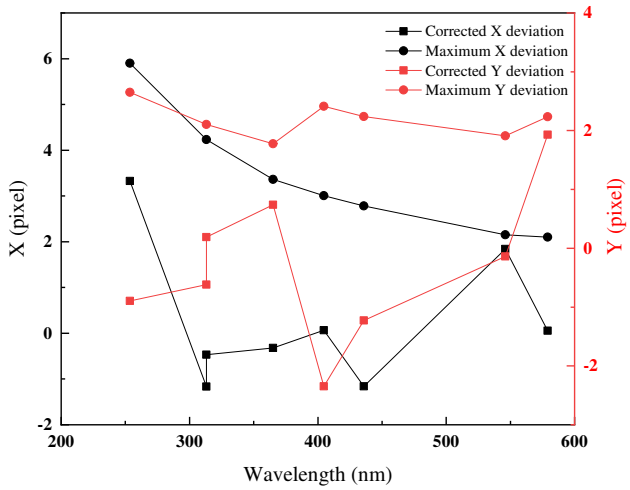

Fig. 9. Comparison between the deviation of corrected spectral reduction model and maximum deviation.

the deviation between the corrected coordinates and the actual coordinates with the deviation between the theoretical coordinates and the actual coordinates, it is found that the correction of the initial model can effectively reduce the deviation as a whole. (2) The error of x coordinates will result in the wrong extraction of order. The deviation of x coordinates between corrected coordinates and actual coordinates of the eight wavelengths is less than half of the corresponding interval pixels between adjacent orders, which means the wrong extraction of order will not appear. (3) The error of y coordinates will affect the accuracy of the wavelength extraction. The design value of the spectral resolution in short, medium, and long wavelengths is 0.01, 0.015, and 0.02 nm, respectively. The pixel resolution of different orders is shown in column 6. Therefore, the deviation of y coordinates between the corrected coordinates and the actual coordinates of the eight wavelengths multiplied by the corresponding pixel resolution is less than the spectral resolution. It is determined that the corrected spectral reduction model satisfies the requirement of wavelength extraction.

6. CONCLUSION

The spectral reduction model for the echelle spectrometer based on a DMD and PMT is established. The relationship between the wavelengths and corresponding coordinates on the DMD is obtained by establishing the mathematical models of the imaging mirror and the lens group. In order to further improve the accuracy of the initial reduction model, the refractive index of the prism is fitted, and the coordinate expressions are calibrated according to the known wavelengths and corresponding coordinates. The accuracy of the corrected spectral reduction model is verified by a two-dimensional spectrogram of a mercury lamp, which satisfies the requirement of extraction of the order and wavelength for the spectrometer. The established echelle spectrometer combined the DMD as spatial light modulator and PMT for detection has the characteristics of wide wavelength range and high resolution. The mode of the block scanning of DMD without collecting the entire spectral information makes the detection flexible. This echelle spectrometer can be further used for qualitative and quantitative analysis of elements in spectrometric instruments.

Funding. National Key Research and Development Program of China (2016YFF0103303).

Disclosures. The authors declare no conflicts of interest.

Data Availability. Data underlying the results presented in this paper are not publicly available at this time but may be obtained from the authors upon reasonable request.

REFERENCES

1. S. V. Bykov, B. Sharma, and S. A. Asher, "High-throughput, high-resolution echelle deep-UV Raman spectrometer," Appl. Spectrosc. **67**, 873–883 (2013).
2. T. W. Barnard, M. I. Crockett, J. C. Ivaldi, and P. L. Lundberg, "Design and evaluation of an echelle grating optical system for ICP-OES," Anal. Chem. **65**, 1225–1230 (1993).
3. M. Shen, Z. Hao, X. Li, C. Li, L. Guo, Y. Tang, P. Yang, X. Zeng, and Y. Lu, "New spectral reduction algorithm for echelle spectrometer in laser-induced breakdown spectroscopy," Opt. Express **26**, 34131–34141 (2018).
4. H. Becker-Ross, M. Okruss, S. Florek, U. Heitmann, and M. D. Huang, "Echelle-spectrograph as a tool for studies of structured background in flame atomic absorption spectrometry," Spectrochim. Acta B Atom. Spectros. **57**, 1493–1504 (2002).
5. D. Ganziy, B. Rose, and O. Bang, "Compact multichannel MEMS based spectrometer for FBG sensing," Proc. SPIE **10323**, 103230B (2017).
6. N. T. Quyen, E. Da Silva, N. Q. Dao, and M. D. Jouan, "New Raman spectrometer using a digital micromirror device and a photomultiplier tube detector for rapid on-line industrial analysis. Part I. Description of the prototype and preliminary results," Appl. Spectrosc. **62**, 273–278 (2008).
7. C. Tao, C. S. Li, Y. C. Li, H. X. Wang, Y. R. Zhang, Z. H. Zhou, X. F. Mao, Z. Y. Ma, and D. Tian, "A UV digital micromirror spectrometer for

dispersive AFS: spectral interference in simultaneous determination of Se and Pb," J. Anal. At. Spectrom. **34**, 413–414 (2019).
8. T. M. Spudich, C. K. Utz, J. M. Kuntz, R. A. Deverse, R. M. Hammaker, and D. L. Mccurdy, "Potential for using a digital micromirror device as a signal multiplexer in visible spectroscopy," Appl. Spectrosc. **57**, 733–736 (2003).
9. E. P. Wagner, B. W. Smith, S. Madden, J. D. Winefordner, and M. Mignardi, "Construction and evaluation of a visible spectrometer using digital micromirror spatial light modulation," Appl. Spectrosc. **49**, 1715–1719 (1995).
10. N. T. Quyen, M. D. Jouan, N. Q. Dao, S. E. Da, and P. D. Ai, "New Raman spectrometer using a digital micromirror device and a photomultiplier tube detector for rapid on-line industrial analysis. Part II. Choice of analytical methods," Appl. Spectrosc. **62**, 279–284 (2008).
11. R. Zhang, M. Z. Pan, J. Yang, Bayanheshig, and J. C. Cui, "Optical system of echelle spectrometer based on DMD," Opt. Precis. Eng. **25**, 2994–3000 (2017).
12. J. Frank, L. Moore, and B. Furst, "Echelle calibration and wavelength calculation," J. Opt. Soc. Am. **62**, 762–766 (1972).
13. D. A. Sadler, D. Littlejohn, and C. V. Perkins, "Automatic wavelength calibration procedure for use with an optical spectrometer and array detector," J. Anal. At. Spectrom. **10**, 253–257 (1995).
14. P. Ballester and M. R. Rosa, "Modeling echelle spectrographs," Astron. Astrophys. Suppl. Ser. **126**, 563–571 (1997).
15. K. Liu and G. M. Hieftje, "Investigation of wavelength calibration for an echelle cross-dispersion spectrometer," J. Anal. At. Spectrom. **18**, 1177–1184 (2003).
16. F. Duan, Y. Qin, X. Fu, L. Ma, T. Huang, and C. Zhang, "Simple spectral reduction algorithm used for the echelle spectrometer," Appl. Opt. **57**, 8921–8927 (2018).
17. S. C. Zhu Jiwei, Y. Jin, M. Tingting, G. Xueqiang, and Z. Jian, "Spectrogram reduction for echelle grating spectrometer based on polynomial fitting," Opt. Precis. Eng. **28**, 1627–1633 (2020).
18. J. J. Mcneill, "Wavelength measurement in echelle spectra," J. Opt. Soc. Am. **49**, 441–444 (1959).
19. N. A. Finkelstein, "The measurement of wavelength in echelle spectra," J. Opt. Soc. Am. **43**, 90 (1953).
20. S. C. Y. Tang, Bayanheshig, J. Cui, and J. Chen, "Spectral reducing of cross-dispersed echelle spectrograph and its wavelength calibration," Opt. Precis. Eng. **18**, 2130–2136 (2010).
21. R. Zhang, Bayanheshig, L. Yin, X. Li, J. Cui, J. Yang, and C. Sun, "Wavelength calibration model for prism-type echelle spectrometer by reversely solving prism's refractive index in real time," Appl. Opt. **55**, 4153–4158 (2016).
22. R. Zhang, Bayanheshig, X. Li, and J. Cui, "Establishment and correction of an echelle cross-prism spectrogram reduction model," Opt. Commun. **403**, 401–407 (2017).
23. L. Yin, Bayanheshig, J. Yang, Y. X. Lu, R. Zhang, C. Sun, and J. C. Cui, "High-accuracy spectral reduction algorithm for the echelle spectrometer," Appl. Opt. **55**, 3574–3581 (2016).